

DIRAS2 promotes radiation resistance in renal cell carcinoma via autophagy induction and MKK4-JNK1 pathway activation

C.F. Cai^{1,2}, Y. He², D. Yue³, Z.H Wang¹, N. Guo^{1,4}, J. Tian^{1,4*}

¹Department of Urology, Qilu Hospital, Cheeloo College of Medicine, Shandong University, Jinan 250014, Shandong, China

²Laboratory of Basic Medical Sciences, Qilu Hospital, Cheeloo College of Medicine, Shandong University, Jinan 250014, Shandong, China

³Department of Urology, Affiliated Hospital of Jining Medical University, Jining 272000, Shandong, China

⁴Department of Organ Transplantation, Qilu Hospital, Cheeloo College of Medicine, Shandong University, Jinan 250014, Shandong, China

ABSTRACT

► Original article

*Corresponding author:

Jun Tian, Ph.D.

E-mail:

198862000666@email.sdu.edu.cn

Received: April 2022

Final revised: February 2023

Accepted: February 2023

Int. J. Radiat. Res., October 2023;
21(4): 805-813

DOI: 10.52547/ijrr.21.4.28

Background: To investigate the effect of DIRAS2 on the response to ionizing radiation (IR) and the related potential molecular mechanism in human ccRCC cells. **Materials and Methods:** In this paper, the expression levels of DIRAS2 in human ccRCC and paired normal tissues were obtained from the Oncomine platform and The Cancer Genome Atlas (TCGA) database, which was further validated by immunohistochemistry. DIRAS2-overexpression cell lines were constructed using a lentivirus-mediated gene expression system. A clonogenic assay was performed to evaluate cell radiation resistance. The effect of DIRAS2 on autophagy was determined by immunoblotting and immunofluorescence analysis. The expression of DIRAS2 and related signalling molecules was evaluated by immunoblotting. **Results:** Here, we found that the expression of DIRAS2 was upregulated in human ccRCC. Overexpression of DIRAS2 promoted radiation resistance in ccRCC cells and enhanced the levels of radiation-induced autophagy. Moreover, inhibition of autophagy by chloroquine (CQ) pretreatment largely eliminated the effect of DIRAS2 overexpression on radiation resistance. Finally, molecular mechanism investigation showed that DIRAS2 activated the mitogen-activated protein kinase (MAPK) kinase 4 (MKK4)-c-Jun NH2-terminal kinase 1 (JNK1)-Bcl-2 pathway. **Conclusion:** Taken together, these results indicated that DIRAS2 may confer radiation resistance to human RCC via autophagy induction through the MKK4-JNK1-Bcl-2 signalling pathway.

Keywords: Clear cell renal cell carcinoma, DIRAS2, autophagy, radiation resistance.

INTRODUCTION

Worldwide, renal cell carcinoma (RCC) is the 7th most common tumour in men and the 9th most common tumour in women and accounts for ~2–3% of all adult malignancies (1–3). RCC encompasses a variety of tumours originating from renal tubular epithelial cells (4), while clear cell renal cell carcinoma (ccRCC) is the most common subtype of RCC and has the highest lethality rate. Indeed, the majority (83% to 88%) of metastatic RCC is histologically ccRCC (5–6). Surgical treatment is the first choice for RCC patients with localized or oligometastatic disease (7). Radiotherapy (RT) is an effective and promising treatment strategy for solid tumours. However, RCC has been historically considered a radioresistant malignancy, and radiation resistance has been regarded as the main obstacle to improving the definitive treatment of RCC (8). There is an urgent need to explore the mechanism underlying the radiation resistance of RCC to achieve the routine use of radiotherapy in clinical RCC patients.

GTP-binding Ras-like protein 2 (DIRAS2) is a member of a distinct subgroup of the Ras family. Despite its similarity in sequence, DIRAS2 differs from other Ras family members in biochemical and functional properties (9–10). DIRAS2 is normally expressed predominantly in the brain and was originally studied in attention deficit/hyperactivity disorders (ADHDs) (11). In recent years, it has also been reported that DIRAS2 may be involved in tumour progression. DIRAS2 has been shown to be potentially carcinogenic in ccRCC as an activator of the mitogen-activated protein kinase (MAPK) signalling pathway in the absence of the von Hippel-Lindau protein (pVHL) (12). In ovarian cancer, DIRAS2 was found to be downregulated and associated with reduced overall and disease-free survival. In murine ovarian cancer cells, DIRAS2 induced cell death via autophagy (10). To date, there is no report on the role of DIRAS2 in radiation resistance.

Macroautophagy (hereafter referred to as autophagy) is a catabolic process responsible for

removing long-lived proteins, misfolded proteins and damaged organelles, which maintains intracellular homeostasis⁽¹³⁾. It is conventionally considered that autophagy plays a protective role against various forms of stress, such as ionizing radiation (IR)⁽¹⁴⁾, although autophagy was also reported to act in a cytotoxic fashion in response to radiotherapy⁽¹⁵⁾. Signal transduction regulated by mammalian target of rapamycin (mTOR), autophagy-related protein Beclin-1 and mitogen-activated protein kinase (MAPK)/c-Jun NH2-terminal kinase (JNK) has been confirmed to play important roles in the autophagy process⁽¹⁶⁾. The relationship between autophagy and radiation resistance has been widely investigated, but more in-depth explorations of the mechanisms are needed to explain the paradoxical role of autophagy in the response to radiation.

In this study, we mainly aimed to investigate the exact role of DIRAS2 in the regulation of radiation resistance in ccRCC. In addition, we also studied the underlying mechanism involving autophagy and related signalling pathways.

MATERIAL AND METHODS

Cell lines and culture conditions

Human RCC cell lines, 786-O and A498 were purchased from the Procell Life Science & Technology Co., Ltd., China. The cells were, respectively, maintained in Roswell Park Memorial Institute (RPMI) 1640 medium and Dulbecco's modified eagle's medium (DMEM) (Gibco, Life Technologies Inc. USA) supplemented with 10% fetal bovine serum (FBS) (Lonsera, S711-001S, Uruguay), 1% penicillin-streptomycin (10,000 U/ml penicillin and 10 mg/ml streptomycin, Gibco, Life Technologies Inc., cat#15140122, USA). All cells lines were cultured at 37 °C in humidified atmosphere containing 5% CO₂. The medium was replaced 2–3 times every week.

Cell transfection

The Lentivirus-based DIRAS2 overexpression system was purchased from GenePharma Company (Shanghai, China). The Flag tag was fused to the C-terminus of DIRAS2. The lentivirus overexpressing DIRAS2 and negative control lentivirus were employed to infect the human ccRCC cell lines 786-O and A498. The stable infection cells were selected with 4 µg/ml puromycin (Solarbio, P8230, China). The transfection efficiency was verified by qRT-PCR and western blotting.

Quantitative real-time PCR (qRT-PCR)

Total RNA was extracted from cultured cells using RNA-Quick Purification Kit (Esunbio, RN001, China) pursuant to the manufacturer's guidelines. Then, the concentration and purity of extracted RNA were

determined by a DS 11 Spectrophotometer (DeNovix, USA). The total RNA was then reverse transcribed to cDNA using a FastKing RT Kit (with gDNase) (TIANGEN BIOTECH, KR116, China), and then detected by qRT-PCR with a SYBR Green Real-time PCR Master Mix (Thermo, #4385610, USA). The primer sequences are shown in Table 1. The relative mRNA expression levels were calculated using the 2^{-ΔΔCT} method. The relative abundance of mRNA was calculated by normalization to GAPDH.

Table 1. Primer sequences in qRT-PCR.

Target gene	Strand	Primer sequence
GAPDH	Forward	5'GCACCGTCAAGGCTGAGAAC3'
	Reverse	5'TGGTGAAGACGCCAGTGGAA3'
DIRAS2	Forward	5'TTGCAGATCACCGACACGAC3'
	Reverse	5'CTGTCCGGCTGGTAATGGAGT3'

Protein extraction and western blotting

Cells were lysed with RIPA lysis buffer (Solarbio, R0010, China) supplemented with PMSF (1%, v/v) (Solarbio, P0100, China). The protein concentration was measured using an Enhanced BCA Protein Assay Kit (Beyotime, P0010S, China). From each sample, 40 µg of total protein was separated by 8–12% sodium dodecyl sulfate-polyacrylamide gels (SDS-PAGE) and transferred onto hydrophobic PVDF membrane (Millipore, IPVH00005, USA). Membranes were blocked in 5% skim milk powder in TBS (Solarbio, T1083, China) containing Tween 20 (Solarbio, T8280, China). (0.1%, v/v) for 1 h at room temperature, and then incubated with primary antibodies overnight at 4 °C. Following the primary antibody incubation, the membranes were washed in TBST and incubated with HRP-conjugated secondary antibody (CST, #7076(Mouse)/#7074(Rabbit), USA) for 1 h at room temperature. The protein bands were detected by ECL reagent (Millipore, WBKLS0100, USA) and quantified by Image J (National Institutes of Health).

Primary antibodies against GAPDH (Abcam, ab181603, UK) and JNK (Abcam, ab199380, UK) were purchased from Abcam. Primary antibodies against DIRAS2 (Origene, TA809398, China) were purchased from Origene. Primary antibodies against Bcl-2 (Affinity, AF6139, Chian), p-Bcl-2 (Affinity, AF3138, China), were purchased from Affinity. Primary antibodies against FLAG (CST, #14793, USA), SQSTM1/P62 (CST, #5114, USA), LC3B (CST, #3868, USA), p-SAPK/JNK (CST, #4668, USA), SEK1/MKK4 (CST, #9152, USA), P-SEK1/MKK4 (CST, #4514, USA), P38 MAPK (CST, #8690, USA) and p-P38 MAPK (CST, #8690, USA) were purchased from Cell Signaling Technology Inc. HRP-linked secondary antibodies directed against rabbit or mouse IgG, respectively, were purchased from Cell Signaling Technology Inc.

Patient samples

Clinical and molecular information for ccRCC samples was obtained from the TCGA dataset.

Transcriptional level analysis of DIRAS2 gene based on Oncomine database was performed on three independent data sets, Jones Renal, Gumz Renaland Lenburg Renal.

Fresh samples of human ccRCC tissue and six paired normal tissue were obtained during surgery at the Department of urinary surgery, Qilu Hospital of Shandong University, China. All samples were collected with the informed consent of patients and the study was approved by the Ethics Committee of Qilu Hospital of Shandong University (Registry number 2012021014).

Immunohistochemistry (IHC)

The human ccRCC tissues obtained from the operation were fixed in 10% formaldehyde (Servicebio, G1101-500ML, China) for 24 hours and then embedded in paraffin. The paraffin slices were prepared, deparaffinized, rehydrated, and treated with 0.01 M sodium citrate (pH 6.0) (Servicebio, G1202-250ML, China) for 20 min at 98 °C for antigen retrieval. Then, endogenous peroxidase activity was blocked with H₂O₂ (0.3%, v/v) in distilled water, and goat serum (Servicebio, G1208-5ML, China) in PBS (10%, v/v) was used to block non-specific antigens. Subsequently, the slices were incubated with a mouse polyclonal DIRAS2 antibody (Origene, TA809398, China), diluted in 1% goat serum (1:500) (Servicebio, G1208-5ML, China) at 4 °C overnight. After incubation with horseradish peroxidase (HRP)-conjugated secondary antibody (CST, #7076(Mouse)/#7074 (Rabbit), USA) for 1h at room temperature, slices were incubated with 3,3'-diaminobenzidine (DAB, 25mg/ml) (Servicebio, G1212-200T, China) for 10 min. All tissue slices were counterstained with hematoxylin (Servicebio, G1104-100ML, China). Stained slides were viewed under the OLYMPUS DP27 microscope and analyzed by Image J.

Immunofluorescence

Cells on coverslips were fixed with methanol and blocked with goat serum (Origene, ZLI-9022, China). The cells were then incubated with the primary antibody against LC3B (CST, #3868, USA) at 4 °C overnight. After rinsing with PBS, coverslips were incubated with DyLight® 488, Goat Anti-Rabbit IgG (1:500, Abbkine, A23220, China), and the cell nuclei were stained with DAPI solution (Solarbio, C0065, China) for visualization. Three fields from each coverslip were randomly captured with Olympus DP72, and three independent experiments were performed. Quantification of LC3 puncta base on the fluorescence intensity was calculated with Image J.

Clonogenic survival assay

Cells were trypsinized to generate single-cell suspensions and seeded in six-well plates at 1000 cells per well. Then the cells were exposed to different doses of radiation (0 Gy, 2 Gy, 4 Gy, 6Gy) by a medical linear accelerator (varian 23 EX, USA).

After culture for 7-14 days to allow cell colony formation, the cells were fixed in ethanol and stained with crystal violet for half an hour. Only colonies containing more than 50 wells were counted. The adherence rate was referred to the ratio comparing the number of colonies formed to the number of cells planted. Survival fraction (SF) is referred to the adherence rate at each dose divided by that at 0 Gy. The colony formation ability means the ratio of the SF of the transfected cells to the control cells under the same dose of radiation. The survival curves were calculated with Prism 7.0 (GraphPad Inc., La Jolla, CA, USA). The mean lethal dose (D₀), quasi-threshold dose (D_q), and survival fractions at 2 Gy (SF₂) were calculated by fitting the survival curves into the single-hit multitarget model ($y=1-[1-e^{(-kx)}]^N$).

Statistical analysis

The statistical analyses were performed using the GraphPad Prism software (GraphPad Software Inc., La Jolla, CA). For each experiment, at least three biological replicates were conducted, and data are expressed as mean ± SD, unless otherwise specified. Statistical significance was analyzed using a two-tailed Student's t-test or repeated measures ANOVA. Values of P < 0.05 were considered statistically significant.

RESULTS

DIRAS2 is highly expressed in human ccRCC

To investigate the role of DIRAS2 in radiation resistance, we explored the expression of DIRAS2 in human ccRCC. First, the Oncomine platform and The Cancer Genome Atlas (TCGA) database were used to analyse the transcriptional expression of DIRAS2 in different types of human cancers, mainly ccRCC. As shown in figure 1a-e, compared with the adjacent normal kidney tissue samples, the mRNA levels of DIRAS2 were significantly higher in ccRCC tissues. To verify the expression differences in the databases, we performed immunohistochemical experiments on paired ccRCC specimens, and the results in figure 1f show that DIRAS2 was highly expressed in tumour tissues. These data all indicated that DIRAS2 expression was upregulated in ccRCC and whether upregulated DIRAS2 expression is involved in radiation resistance of ccRCC was further studied.

DIRAS2 promotes radiation resistance of ccRCC cells

To better understand the role of DIRAS2 in radiation resistance of ccRCC in vitro, DIRAS2-overexpressing cell lines were constructed by a lentivirus-mediated gene expression system. The 786-O and A498 cells, both of which are von Hippel-Lindau (VHL)-mutated cell lines, were selected to ensure the overexpression of DIRAS2, as the ubiquitination and degradation of DIRAS2 can be

enhanced by pVHL⁽¹²⁾. The Western blot and qRT-PCR results confirmed that DIRAS2 was overexpressed successfully (figure 2a-b). Then, the cells were exposed to different doses of IR. A clonogenic assay was employed to evaluate the effect of DIRAS2 on radiation resistance. As shown in figure 2c, compared with the Lv-NC groups, the survival curves of DIRAS2 OV cells shifted upwards significantly in both 786-0 and A498 cell lines. The

mean lethal dose (D0), quasi-threshold dose (Dq), and survival fractions at 2 Gy (SF2) were also calculated based on a clonogenic assay. DIRAS2-OV cells had higher values of D0, Dq and SF2 (all $p < 0.05$) than Lv-NC cells (figure 2d). DIRAS2 OV groups had more colonies to survive than Lv-NC cells under the same dose of IR (4 Gy) (figure 2e). These results suggested that upregulated expression of DIRAS2 conferred radiation resistance in human ccRCC cells.

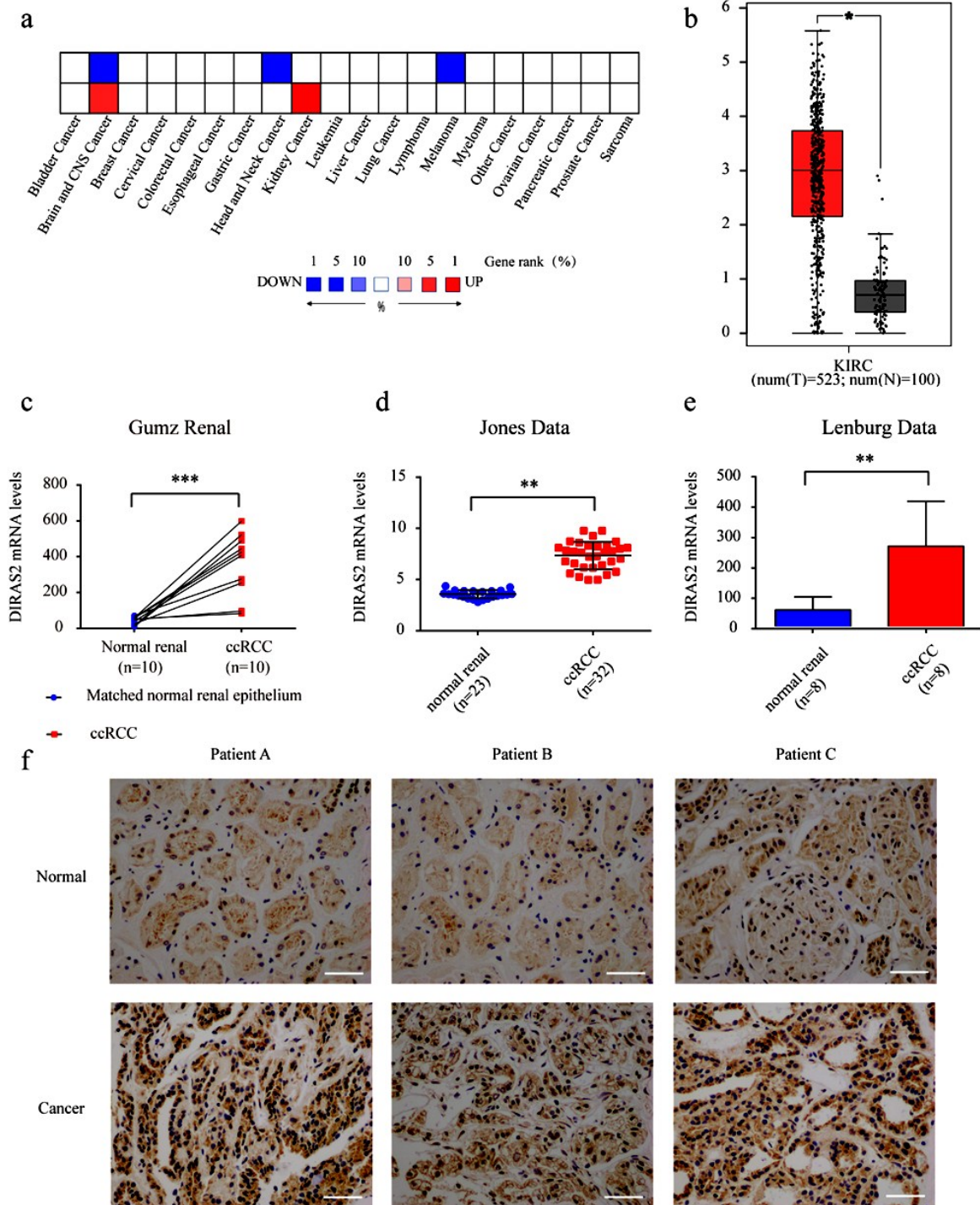


Figure 1. DIRAS2 is highly expressed in human ccRCC. Analysis of DIRAS2 expression in different cancer types from the Oncomine (a) and TCGA databases (b). (c)-(e) Analysis of DIRAS2 expression in ccRCC versus normal tissues in three independent datasets from the Oncomine database. *, $p < 0.05$; **, $p < 0.01$ and ***, $p < 0.001$. (f) Immunohistochemical staining of DIRAS2 expression in human ccRCC samples and normal tissues. Scale bar 100 μm .

[Downloaded from ijrr.com on 2026-05-16] [DOI: 10.61186/ijrr.21.4.805]

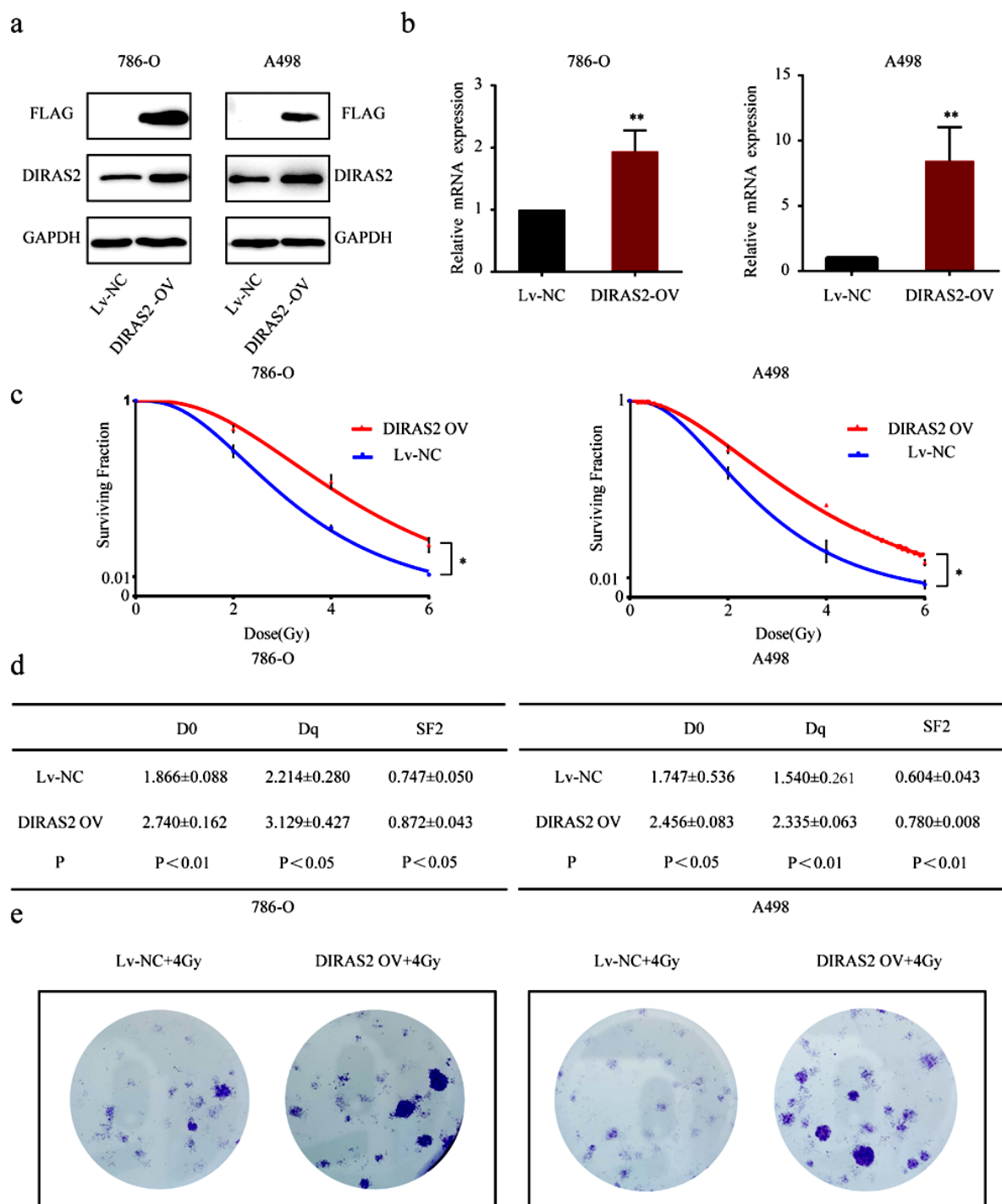


Figure 2. Overexpression of DIRAS2 increases radiation resistance in ccRCC cell lines. The expression levels of DIRAS2 in 786-O and A498 cells transfected with DIRAS2 OV and Lv-NC lentivirus were verified by Western blotting (a) and qRT-PCR (b). (c) The effect of DIRAS2 overexpression on radiosensitivity of 786-O and A498 cells measured by clonogenic survival assay. Cells were subjected to the indicated doses of IR (0, 2, 4, 6 Gy). (d) The mean lethal dose (D0), quasi-threshold dose (Dq), and survival fractions at 2 Gy (SF2) were calculated using the single-hit multitarget model. The D0, Dq, and SF2 values of the DIRAS2 OV groups were higher than those of the Lv-NC groups, indicating the enhancement effect of DIRAS2 on radiation resistance in 786-O and A498 cells. (e) Colony formation of transfected 786-O and A498 cells exposed to 4 Gy radiation. These data are expressed as the mean \pm SD of three biological replicates (*, $p < 0.05$ and **, $p < 0.01$.)

Human ccRCC cells overexpressing DIRAS2 exhibit enhanced autophagy in response to IR

Since it has been reported that autophagy may play a prosurvival role under various stress conditions (17-19), including ionizing radiation (20), we overexpressed DIRAS2 in the 786-O and A498 cell lines and measured the expression levels of the

autophagy-related marker LC3. Compared with LC3-II, LC3-I was less sensitive to antibodies and more prone to degradation under repeated freeze-thaw conditions, so the LC3-II/GAPDH method was adopted in this experiment (21). In addition, a positive control group with the addition of the autophagy inhibitor chloroquine (CQ), which blocks autophagic

flux by regulating the pH value of lysosomes, was established to further reflect the changes in autophagy. As shown in figure 3A, in both the Lv-NC and DIRAS2-OV groups, after IR (6 Gy) treatment, LC3-II levels increased, and the peak values were reached before 8 h after IR treatment. However, overexpression of DIRAS2 promoted the conversion of LC3-I to LC3-II in both 786-O and A498 cells, and the LC3-II levels increased more significantly in the DIRAS2-OV groups than in the Lv-NC groups (figure 3a). Furthermore, measurements of autophagy were visualized by immunofluorescence of LC3-II. As shown in figure 3b and c, after IR treatment, a largely dispersed fluorescence distribution was observed in the 786-O cells of both the Lv-NC and DIRAS2 groups (figure 3b). Compared with Lv-NC cells, DIRAS2-OV cells exhibited more intense LC3-II-associated red fluorescence puncta (figure 3b), and the number of LC3 fluorescent puncta dramatically increased in DIRAS2-OV cells (figure 3c). Consistent results were obtained in A498 cells, as shown in figure S1. In conclusion, our data demonstrate that overexpression of DIRAS2 can upregulate the autophagy level in human ccRCC cells, which is more obvious after IR treatment, suggesting that DIRAS2-enhanced autophagy may be related to radiation resistance.

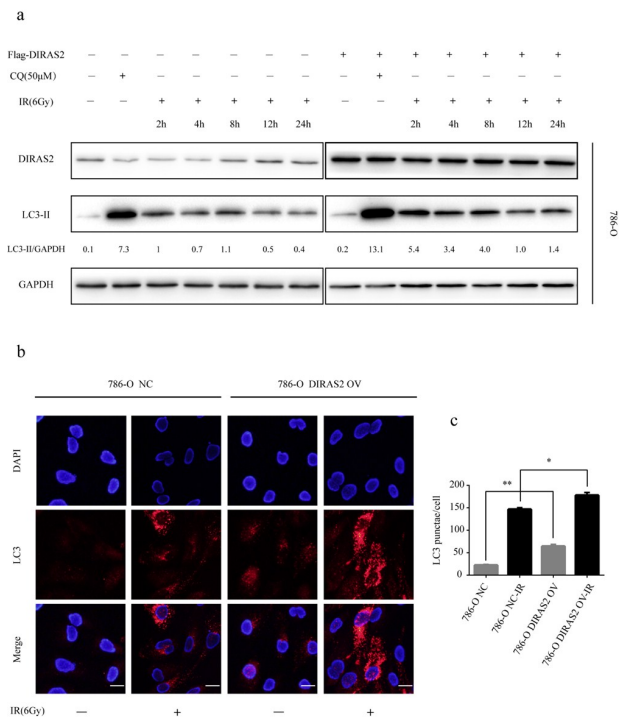


Figure 3. DIRAS2 overexpression enhances autophagy in response to ionizing radiation in ccRCC cells 786-O cells overexpressing DIRAS2 (DIRAS2-OV) and control cells (Lv-NC) were treated with or without IR (6 Gy), and the cell lysate was collected at the indicated time points after IR. (a) The protein levels of DIRAS2 and LC3-II were determined by Western blot analysis. The ratios of LC3-II/GAPDH were calculated by greyscale value analysis. (b) Laser confocal microscopy images showing LC3 staining in the DIRAS2-OV and Lv-NC groups of 786-O cells labelled with fluorescent antibodies against LC3 (red channel) at 2 hours post-IR or mock treatment. Nuclear stained DAPI (blue channel). Scale bar 20 μm. (c) Quantification of LC3 puncta from the images in (b). Data are shown as the mean ± SD of three replicates. *, p < 0.05, and **, p < 0.01

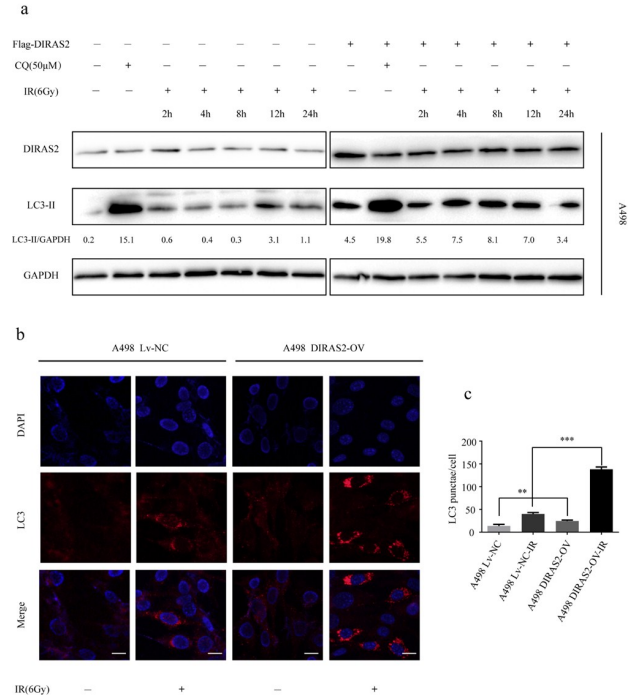


Figure S1. DIRAS2 overexpression enhances autophagy in response to ionizing radiation in ccRCC cells A498 cells overexpressing DIRAS2 (DIRAS2-OV) and control cells (Lv-NC) were treated with or without IR (6 Gy), and the cell lysate was collected at the indicated time points after IR. (a) The protein levels of DIRAS2 and LC3-II were determined by Western blot analysis. The ratios of LC3-II/GAPDH were calculated by greyscale value analysis. (b) Laser confocal microscopy images showing LC3 staining in the DIRAS2-OV and Lv-NC groups of A498 cells labelled with fluorescent antibodies against LC3 (red channel) at 2 hours post-IR or mock treatment. Nuclear stained DAPI (blue channel). Scale bar 20 μm. (c) Quantification of LC3 puncta from the images in (b). Data are shown as the mean ± SD of three replicates. **, p < 0.01, and ***, p < 0.001.

Inhibition of autophagy can eliminate the effect of DIRAS2 overexpression on radiation resistance in human ccRCC cells

Because DIRAS2 overexpression induced autophagy and enhanced the level of autophagy in response to ionizing radiation, we attempted to explore whether autophagy plays a critical role in radiation resistance induced by DIRAS2 overexpression in human ccRCC cells. The DIRAS2-OV and Lv-NC groups of 786-O and A498 cells were treated with the autophagy inhibitor chloroquine (CQ) for 12 h before exposure to different doses of IR. As shown in figure 4a, DIRAS2 overexpression was verified by western blot analysis with anti-FLAG and anti-DIRAS2 antibodies. To confirm autophagy inhibition, the levels of both LC3-II and P62 increased significantly compared with those in the untreated control groups (figure 4a), which suggested that autophagic flux was successfully blocked. To assess the cell radiation sensitivity, a clonogenic assay was performed, and the survival curves are shown in figure 4b. Only a marginal difference was observed between the Lv-NC group cells with or without CQ treatment. Consistent with the results above, DIRAS2-OV groups were significantly more resistant to IR compared with Lv-NC groups in both 786-o and A498

cell lines. However, under CQ treatment, the survival curves of the DIRAS2-OV groups shifted downwards significantly (figure 4b). Moreover, D0, Dq and SF2 were also calculated (figure 4c). DIRAS2-OV cells had higher values of D0, Dq and SF2 than Lv-NC cells. After pretreatment with CQ, the values of D0, Dq, and SF2 of DIRAS2-OV cells were reduced and were not significantly different from the values of Lv-NC cells without CQ treatment. Taken together, our data show that autophagy inhibition sensitized DIRAS2-OV cells to IR, indicating that DIRAS2 overexpression-induced radiation resistance is at least partially due to enhanced autophagy.

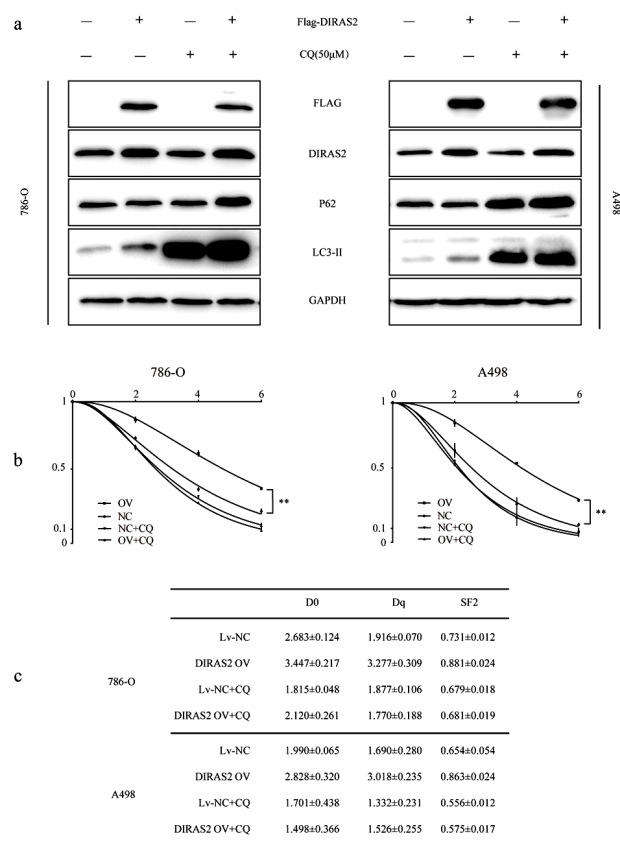


Figure 4. DIRAS2-induced radiation resistance is rescued by pretreatment with the autophagy inhibitor chloroquine (CQ). DIRAS2-OV or Lv-NC 786-O and A498 cells were pretreated with or without 50 μ M CQ for 12 hours and then treated with the indicated doses of ionizing radiation (0, 2, 4, 6 Gy). (a) The overexpression of DIRAS2 and autophagy inhibition were confirmed by Western blot analysis of Flag, DIRAS2, P62 and LC3-II expression. (b) The effect of autophagy inhibition by CQ on radiosensitivity of DIRAS2-OV or Lv-NC cells of 786-O and A498 measured by clonogenic survival assay. (c) The mean lethal dose (D0), quasi-threshold dose (Dq), and survival fractions at 2 Gy (SF2) were calculated using the single-hit multitarget model. Values represent the mean \pm SD of three biological replicates (**, $p < 0.01$).

DIRAS2 enhanced radiation-induced autophagy by activating the MKK4-JNK1 pathway

The activation of the mitogen-activated protein kinase (MAPK) cascade in response to ionizing radiation (IR) plays a critical role in sensitivity to radiation (22). MAPK/c-Jun NH2-terminal kinase (JNK)

has also been associated with the regulation of autophagy (23). Therefore, we performed a Western blot analysis of MAPK signalling activation to investigate the molecular mechanism of DIRAS2 in regulating autophagy in response to radiation. As shown in figure 5, overexpression of DIRAS2 in both 786-O and A498 cells promoted the phosphorylation of MKK4 and JNK1 compared with that in Lv-NC cells. In addition, the DIRAS2 OV cells and the Lv-NC groups were exposed to IR (6 Gy), and MAPK signalling activation in each group was determined (figure 5). After IR, MAPK signalling activation was enhanced in each group, while the levels of phos-MKK4 and phos-JNK1 were both increased in the DIRAS2 OV groups compared with the Lv-NC groups. These data suggest that DIRAS2 may activate MKK4-JNK1 signalling. Furthermore, the phosphorylation level of Bcl-2, which can be phosphorylated by JNK1 and dissociate Beclin1 from the Bcl-2-Beclin 1 complex (24), was upregulated after IR and was also enhanced in the DIRAS2 OV groups compared with the Lv-NC groups (figure 5). These results suggest that DIRAS2 may activate MKK4-JNK1-Bcl-2 signalling, and then phosphorylated Bcl-2 dissociates with Beclin 1 and induces autophagy.

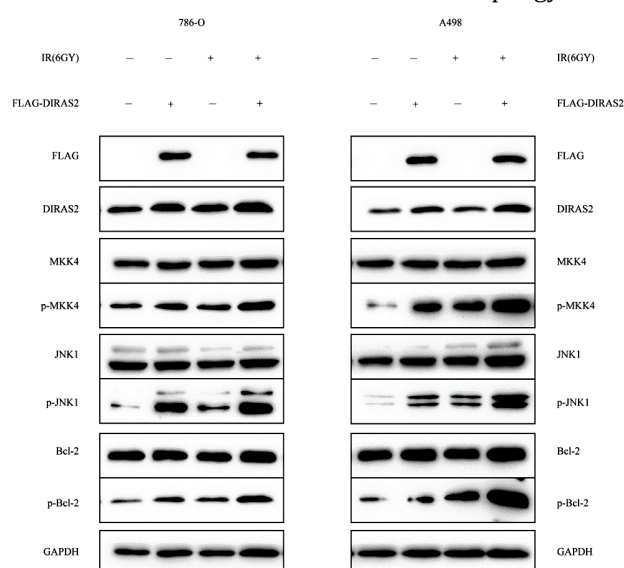


Figure 5. DIRAS2 activates MKK4-JNK1-Bcl-2 signalling in ccRCC cells. The DIRAS2 OV and Lv-NC groups of 786-O and A498 cells were treated with or without IR (6 Gy). The cell lysate was collected 12 h later and subjected to Western blot analysis of Flag, Di-Ras2, MKK4, p-MKK4, JNK1, p-JNK1, Bcl-2, and p-Bcl-2.

DISCUSSION

Ionizing radiation (IR) is an effective therapeutic strategy for the treatment of solid tumours and has been commonly employed by targeting the primary site and especially the postoperative metastatic area. However, the treatment of primary RCC, which presents the vast majority of renal cancer (25), is currently limited to surgical resection, as the

therapeutic effect of radiotherapy for RCC patients is rarely satisfactory. Radiation resistance in RCC cells is the main obstacle limiting the efficacy of radiotherapy. Moreover, normal kidneys around tumours are considered radiation-sensitive, and clinical care should be taken to keep radiation doses within acceptable tolerance limits (26). Therefore, it is necessary to explore the molecular mechanisms underlying the radiation resistance of RCC, which remain largely unknown (27). In the present study, we found that DIRAS2, which was upregulated in ccRCC, contributed to the radiation resistance of RCC by activating MKK4-JNK1 signalling to induce protective autophagy.

A significant proportion of ccRCC is associated with the deletion of the VHL tumour suppressor gene (28), which functions as an E3 ubiquitin ligase complex substrate recognition element to regulate the stability of certain oncogenic-related proteins, including DIRAS2 (12). Thus, a characteristic of VHL-deficient RCCs may be the production of high levels of DIRAS2 due to their extended intracellular half-life, which is also corroborated by our immunohistochemical results, as it was shown that DIRAS2 was upregulated in human ccRCC. Moreover, DIRAS2 plays a carcinogenic role in ccRCC formation by promoting cell proliferation, migration and invasion (12). However, DIRAS2 is rarely studied in human tumours, and to our knowledge, the role of DIRAS2 in the radiation response has not been demonstrated. In this study, we found that overexpression of DIRAS2 markedly enhanced colony formation of ccRCC cells under IR, suggesting that DIRAS2 may contribute to radiation resistance.

DIRAS2 was required for autophagy in murine ovarian cancer cells (10). Based on gene homology, we speculated that DIRAS2 also regulated autophagy in human ccRCC cells, which was confirmed in the present study. It should be noted that autophagy induced in response to IR treatment may play a cytoprotective role against stress but does not represent a mechanism of radiation resistance (29). It has been reported that inhibition of autophagy with CQ and Lys01 or by deletion of autophagy-related 7 (ATG7) does not alter the sensitivity of KRAS mutant tumours to radiation in vitro and *in-vivo* (30). Our results demonstrated higher basal autophagy in the human ccRCC cell lines overexpressing DIRAS2 compared to the transfection control groups even without IR treatment. Moreover, with the pretreatment of cells with CQ for autophagy inhibition, the radiation resistance of the DIRAS2 OV group was weakened, and there was no significant difference between the survival curves of the DIRAS2 OV group and the Lv-NC group. The durable higher basal autophagy may contribute to the radiation resistance of ccRCC cells here.

Next, we explored the relationship between DIRAS2 and signalling pathways related to

autophagy. The Ras-MAPK signalling pathway is one of the classic oncogenic pathways (31-32), and DIRAS2 has also been proven to activate the RAS-MAPK pathway in VHL-deficient ccRCC cell lines (12). In addition, the activation of JNK1 in the MAPK family has also been confirmed to be related to stress stimulation, including IR (24). Western blot results showed that DIRAS2 could indeed activate the MKK4-JNK1 signalling pathway, and the phosphorylation of Bcl-2 induced by JNK1 promoted the dissociation of the Bcl-2/Beclin 1 complex, which enhanced autophagy (29).

In conclusion, our study revealed for the first time that DIRAS2 can trigger autophagy and activate MKK4-JNK1 signalling in human ccRCC cells and that DIRAS2-induced autophagy plays a cytoprotective role and contributes to radiation resistance. The tumour microenvironment plays pivotal roles in determining radiotherapy outcomes; thus, comprehensive and systematic clinical data and *in vivo* experiments are required to further evaluate the role of DIRAS2 and autophagy in the radiation resistance of RCC.

CONCLUSION

Taken together, these results indicated that DIRAS2 may confer radiation resistance to human RCC via autophagy induction through the MKK4-JNK1-Bcl-2 signalling pathway.

ACKNOWLEDGEMENTS

We thank the Department of Radiation Oncology of Qilu Hospital for providing equipment and technical support for this experiment.

Disclosure: The author reports no conflicts of interest in this work.

Ethics Approval: This study was performed in line with the principles of the Declaration of Helsinki. Relevant retrospective studies were conducted on already available biological material, and the study was approved by the Ethics Committee of Qilu Hospital of Shandong University (Registry number 2012021014) .

Funding: No funding was received.

Authors' contributions: All authors made substantial contributions to the conception and design, acquisition of data, or analysis and interpretation of data; took part in drafting the article or revising it critically for important intellectual content; agreed to submit to the current journal; gave final approval of the version to be published; and agree to be accountable for all aspects of the work.

REFERENCES

1. Hsieh JJ, Purdue MP, Signoretti S, *et al.* (2017) Renal cell carcinoma. *Nat Rev Dis Primers*, **3**: 17009.

2. Rini BI, Campbell SC, Escudier B (2009) Renal cell carcinoma. *Lancet*, **373**(9669): 1119-32.
3. Ferlay J, Soerjomataram I, Dikshit R, et al. (2015) Cancer incidence and mortality worldwide: sources, methods and major patterns in GLOBOCAN 2012. *Int J Cancer*, **136**(5): E359-E86.
4. Siegel RL, Miller KD, Jemal A (2017) CA Cancer statistics. *Cancer J Clin*, **67**(1): 7-30.
5. Kroeger N, Xie W, Lee J-L, et al. (2013) Metastatic non-clear cell renal cell carcinoma treated with targeted therapy agents: characterization of survival outcome and application of the International mRCC Database Consortium criteria. *Cancer*, **119**(16): 2999-3006.
6. Vera-Badillo FE, Templeton AJ, Duran I, et al. (2015) Systemic therapy for non-clear cell renal cell carcinomas: a systematic review and meta-analysis. *Eur Urol*, **67**(4): 740-9.
7. Van Poppel H, Da Pozzo L, Albrecht W, et al. (2011) A prospective, randomised EORTC intergroup phase 3 study comparing the oncologic outcome of elective nephron-sparing surgery and radical nephrectomy for low-stage renal cell carcinoma. *Eur Urol*, **59**(4): 543-52.
8. Siva S, Kothari G, Muacevic A, et al. (2017) Radiotherapy for renal cell carcinoma: renaissance of an overlooked approach. *Nat Rev Urol*, **14**(9): 549-63.
9. Gasper R, Sot B, Wittinghofer A (2010) GTPase activity of Di-Ras proteins is stimulated by Rap1GAP proteins. *Small GTPases*, **1**(3): 133-41.
10. Sutton MN, Yang H, Huang GY, et al. (2018) RAS-related GTPases DIRAS1 and DIRAS2 induce autophagic cancer cell death and are required for autophagy in murine ovarian cancer cells. *Autophagy*, **14**(4): 637-53.
11. Reif A, Nguyen TT, Weissflog L, et al. (2011) DIRAS2 is associated with adult ADHD, related traits, and co-morbid disorders. *Neuropsychopharmacology*, **36**(11): 2318-27.
12. Rao H, Li X, Liu M, et al. (2020) Di-Ras2 promotes renal cell carcinoma formation by activating the mitogen-activated protein kinase pathway in the absence of von Hippel-Lindau protein. *Oncogene*, **39**(19): 3853-66.
13. Klionsky DJ, Abdel-Aziz AK, Abdelfatah S, et al. (2021) Guidelines for the use and interpretation of assays for monitoring autophagy (4th edition). *Autophagy*, **17**(1): 1-382
14. Patel NH, Sohal SS, Manjili MH, et al. (2020) The roles of autophagy and senescence in the tumor cell response to radiation. *Radiat Res*, **194**(2):103-15.
15. Kuwahara Y, Oikawa T, Ochiai Y, et al. (2011) Enhancement of autophagy is a potential modality for tumors refractory to radiotherapy. *Cell Death Dis*, **2**: e177.
16. Galluzzi L, Bravo-San Pedro JM, Demaria S, et al. (2017) Activating autophagy to potentiate immunogenic chemotherapy and radiation therapy. *Nat Rev Clin Oncol*, **14**(4): 247-58.
17. Lu J, Cai L, Dai Y, et al. (2021) Polydopamine-based nanoparticles for photothermal therapy/chemotherapy and their synergistic therapy with autophagy inhibitor to promote antitumor treatment. *Chem Rec*, **21**(4): 781-96.
18. Alnasser HA, Guan Q, Zhang F, et al. (2016) Requirement of clusterin expression for prosurvival autophagy in hypoxic kidney tubular epithelial cells. *Am J Physiol Renal Physiol*, **310**(2): F160-F73.
19. Kobara M, Nessa N, Toba H, Nakata T (2021) Induction of autophagy has protective roles in imatinib-induced cardiotoxicity. *Toxicol Rep*, **8**: 1087-97.
20. Chaurasia M, Gupta S, Das A, et al. (2019) Radiation induces EIF2AK3/PERK and ERN1/IRE1 mediated pro-survival autophagy. *Autophagy*, **15**(8): 1391-406.
21. Klionsky DJ, Abdelmohsen K, Abe A, et al. (2016) Guidelines for the use and interpretation of assays for monitoring autophagy (3rd edition). *Autophagy*, **12**(1): 1-222.
22. Lee SY, Jeong EK, Ju MK, et al. (2017) Induction of metastasis, cancer stem cell phenotype, and oncogenic metabolism in cancer cells by ionizing radiation. *Mol Cancer*, **16**(1): 10.
23. Zhou Y-Y, Li Y, Jiang W-Q, Zhou L-F (2015) MAPK/JNK signalling: a potential autophagy regulation pathway. *Biosci Rep*, **35**(3):e00199.
24. Wei Y, Pattingre S, Sinha S, et al. (2008) JNK1-mediated phosphorylation of Bcl-2 regulates starvation-induced autophagy. *Mol Cell*, **30**(6): 678-88.
25. Volpe A and Patard JJ (2010) Prognostic factors in renal cell carcinoma. *World J Urol*, **28**(3): 319-27.
26. De Meerleer G, Khoo V, Escudier B, et al. (2014) Radiotherapy for renal-cell carcinoma. *Lancet Oncol*, **15**(4): e170-e7.
27. Comprehensive molecular characterization of clear cell renal cell carcinoma (2013). *Nature*, **499**(7456): 43-9.
28. Choueiri TK and Kaelin WG (2020) Targeting the HIF2-VEGF axis in renal cell carcinoma. *Nat Med*, **26**(10): 1519-30.
29. Xu H-D and Qin Z-H (2019) Beclin 1, Bcl-2 and autophagy. *Adv Exp Med Biol*, **1206**: 109-26.
30. Eng CH, Wang Z, Tkach D, et al. (2016) Macroautophagy is dispensable for growth of KRAS mutant tumors and chloroquine efficacy. USA. *Proc Natl Acad Sci*, **113**(1): 182-7.
31. Morris MR and Latif F (2017) The epigenetic landscape of renal cancer. *Nat Rev Nephrol*, **13**(1): 47-60.
32. Banumathy G and Cairns P (2010) Signaling pathways in renal cell carcinoma. *Cancer Biol Ther*, **10**(7): 658-64.

